AD-A131 555 ENERGY PARTITIONING TO PRODUCT TRANSLATION IN THE INFRARED MULTIPHOTON DI..(U) CALIFORNIA UNIV BERKELEY DEPT OF CHEMISTRY L J BUTLER ET AL. 07 JUN 83 1/1

UNCLASSIFIED N00014-75-C-0671 F/G 7/4 NL

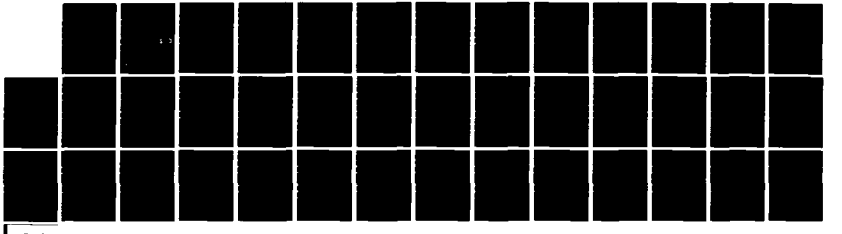

END
FILMED

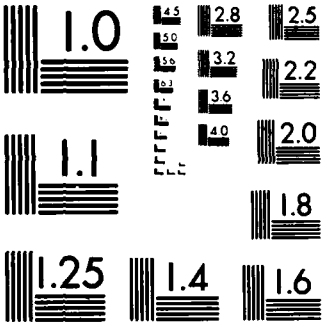

MICROCOPY RESOLUTION TEST CHART
NATIONAL BUREAU OF STANDARDS-1963-A

UNCLASSIFIED

SECURITY CLASSIFICATION OF THIS PAGE (When Data Entered)

(12)

REPORT DOCUMENTATION PAGE	READ INSTRUCTIONS BEFORE COMPLETING FORM
1. REPORT NUMBER: NR 092-545/6/83	2. GOVT ACCESSION NO.: AD A131355
	3. RECIPIENT'S CATALOG NUMBER:
4. TITLE (and Subtitle): ENERGY PARTITIONING TO PRODUCT TRANSLATION IN THE INFRARED MULTIPHOTON DISSOCIATION OF DIETHYL ETHER	5. TYPE OF REPORT & PERIOD COVERED: Technical
	6. PERFORMING ORG. REPORT NUMBER:
7. AUTHOR(s): L. J. Butler, R. J. Buss, R. J. Brudzynski and Y. T. Lee	8. CONTRACT OR GRANT NUMBER(s): N00014-75-C-0671 NR 092-545
9. PERFORMING ORGANIZATION NAME AND ADDRESS: Professor Y.T. Lee, Dept. of Chemistry, University of California, Berkeley, CA 94720	10. PROGRAM ELEMENT, PROJECT, TASK AREA & WORK UNIT NUMBERS:
11. CONTROLLING OFFICE NAME AND ADDRESS: Dr. Richard Miller, Office of Naval Research, Department of the Navy, Code 613A:MAK, 800 N. Quincy Street, Arlington, VA 22217	12. REPORT DATE: June 7, 1983
	13. NUMBER OF PAGES: 38
14. MONITORING AGENCY NAME & ADDRESS (if different from Controlling Office): Mr. Christal C. Grisham, Office of Naval Research Resident Representative, University of California, 239 Campbell Hall, Berkeley, CA 94720	15. SECURITY CLASS. (of this report): UNCLASSIFIED
	15a. DECLASSIFICATION/DOWNGRADING SCHEDULE:

16. DISTRIBUTION STATEMENT (of this Report)

Unlimited

DISTRIBUTION STATEMENT A
Approved for public release;
Distribution Unlimited

DTIC ELECTE AUG 19 1983 S D B

17. DISTRIBUTION STATEMENT (of the abstract entered in Block 20, if different from Report)

18. SUPPLEMENTARY NOTES

Submitted for publication in the Journal of Physical Chemistry.

19. KEY WORDS (Continue on reverse side if necessary and identify by block number)

INFRARED MULTIPHOTON DISSOCIATION
DIETHYL ETHER

20. ABSTRACT (Continue on reverse side if necessary and identify by block number)

The infrared multiphoton decomposition of diethyl ether (DEE) has been investigated by the crossed laser-molecular beam technique. The center-of-mass product translational energy distributions (P(E')) were measured for the two dissociation channels: (1) DEE → C_2H_5O + C_2H_5 and (2) DEE → C_2H_5OH + C_2H_4. The shape of the P(E') measured for the radical channel (1) is in agreement with predictions of statistical unimolecular rate theory. The translational energy released in the concerted reaction (2) peaks at 24 kcal/mole; this exceedingly

(continued on reverse)

DD FORM 1 JAN 73 1473 EDITION OF 1 NOV 65 IS OBSOLETE S/N 0102-LF-014-6601

UNCLASSIFIED
SECURITY CLASSIFICATION OF THIS PAGE (When Data Entered)

AD A131355

DTIC FILE COPY

83 08 18 001

20. Abstract (Continued)

high translational energy release with a relatively narrow distribution results from the recoil of the products from each other down the exit barrier. Applying statistical unimolecular rate theory, the average energy levels from which DEE dissociates to products are estimated using the measured P(E') for the radical channel (1).

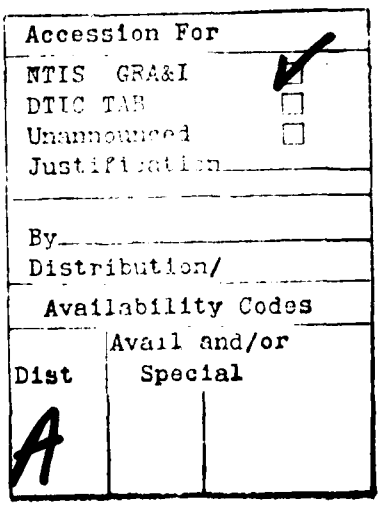

ENERGY PARTITIONING TO PRODUCT TRANSLATION IN THE INFRARED MULTIPHOTON DISSOCIATION OF DIETHYL ETHER

L. J. Butler, R. J. Buss,[a] R. J. Brudzynski and Y. T. Lee

Materials and Molecular Research Division
Lawrence Berkeley Laboratory and
Department of Chemistry, University of California
Berkeley, California 94720 USA

June 1983

ABSTRACT

The infrared multiphoton decomposition of diethyl ether (DEE) has been investigated by the crossed laser-molecular beam technique. The center-of-mass product translational energy distributions (P(E')) were measured for the two dissociation channels: (1) DEE → $C_2H_5O + C_2H_5$ and (2) DEE → $C_2H_5OH + C_2H_4$. The shape of the P(E') measured for the radical channel (1) is in agreement with predictions of statistical unimolecular rate theory. The translational energy released in the concerted reaction (2) peaks at 24 kcal/mole; this exceedingly high translational energy release with a relatively narrow distribution results from the recoil of the products from each other down the exit barrier. Applying statistical unimolecular rate theory, the average energy levels from which DEE dissociates to products are estimated using the measured P(E') for the radical channel (1).

a. present address: Sandia National Laboratory, Division 1811, Albuquerque, New Mexico 87185.

I. INTRODUCTION

Previous molecular beam investigations of unimolecular reaction dynamics have shown that potential energy barriers in the exit channel beyond the endoergicity have a large effect on the asymptotic product translational energy distributions. For almost all of the simple fission reactions studied, in which a single bond is broken without an exit barrier and no new bonds are formed, the products have statistical translational energy distributions.[1] However for all the complex fission reactions studied, in which bonds are broken and formed simultaneously, the translational energy distributions of the products reflect their recoil from each other down the substantial potential energy barrier in the exit channel.[2-4] Huisken et al.[2] studied the infrared multiphoton dissociation (IRMPD) of ethyl vinyl ether (EVE) in a crossed laser-molecular beam apparatus. They observed competition between two dissociation channels: (1) EVE → $CH_3CHO + C_2H_4$ and (2) EVE → $CH_2CHO + C_2H_5$ and found that approximately 70 percent of the 38 kcal/mole exit barrier for reaction (1) was released into product translational energy. Such a high translational energy release, ~30 kcal/mole, in the unimolecular dissociation of a polyatomic molecule in the ground electronic state was previously unsuspected. Several other similar experiments which measured the product translational energy distributions for reactions involving three- and four-center HCl elimination from halogenated hydrocarbons[3] and a three-center Cl_2 elimination from CF_2Cl_2,[4] are reviewed in the paper of Huisken et al. In the four center elimination of hydrogen halides, a large fraction of the exit barrier appears as vibrational excitation of

the products; the average translational energy release does not usually exceed 10 kcal/mole. Also reviewed there are some examples of infrared[5] and laser induced fluorescence[6] techniques used in bulk experiments to measure the internal energy distributions of products from complex fission reactions.

Two groups have independently studied the thermal decomposition of diethyl ether (DEE) and derived preexponential factors and activation energies for the the Arrhenius expression for the rate constants of the primary dissociation processes. Laidler and McKenny[7] and Istvan and Peter[8] both report two competing primary channels, a simple C-O bond fission reaction with little or no exit barrier:

$$CH_3CH_2OCH_2CH_3 \rightarrow C_2H_5O + C_2H_5 \qquad (1)$$

and a molecular elimination reaction with a large exit barrier:

$$CH_3CH_2OCH_2CH_3 \rightarrow C_2H_5OH + C_2H_4 \qquad (2)$$

The Arrhenius parameters for the four-centered elimination (2) were reported to be E_a = 84 kcal/mole and logA = 18.0 by Laidler and McKenny and E_a = 66.0 and logA = 13.9 by Istvan and Peter. The A-factor and activation energy for the radical channel were reported to be 14.0 and 78 kcal/mole respectively by Laidler and McKenny and 14.3 and 77.5 by Istvan and Peter. Benson and O'Neal[9] point out that the Laidler and McKenny A-factors are

not reliable as (2) should have a larger, more positive entropy of activation than rxn. (1) so it is expected that the A factor of (2) is larger than that of (1). They also point out that a fairly reliable estimate for the parameters of the radical reaction (2) can be made from the thermodynamics by assuming a recombination rate of $k_{rec} = 10^{9.7 \pm 1.0}$ l/mol.sec, from which they obtain logA = 16.3 and E_a = 81.8. The other energetically allowed decomposition channels are shown in Fig. 1 along with these two channels. The activation energies shown are those estimated by Benson and O'Neal for the radical channel (1) and reported by Istvan and Peter for the molecular elimination reaction (2).

Thus this system allowed the molecular beam study of two competing dissociation channels, one a concerted reaction with a constrained transition state resulting in a large exit barrier and the other a simple bond fission reaction with a large activation energy but no significant exit barrier. We wished to confirm the identification of these two channels, to investigate the possibility of the occurrence of the other two energetically allowed channels shown in Fig. 1 and to determine the effect of the large exit channel barrier for rxn. (1) on the product translational energy distribution. As will be seen, the velocity distributions of the radical channel products allowed us to determine limits on the energy levels from which the molecules dissociated, thus providing an estimate on the average number of photons absorbed in our IRMPD experiment.

II. EXPERIMENT

Time-of-flight (TOF) distributions of the photofragments were measured in a molecular beam apparatus described in detail elsewhere.[10] The molecular beam was formed by bubbling helium through diethyl ether (DEE) (Mallinckrodt AR grade) maintained at 0°C and expanding the mixture through a 0.005" diameter stainless steel nozzle at a total stagnation pressure of 400 torr (~50 percent DEE/50 percent He). The nozzle was heated to 300°C to eliminate the formation of molecular clusters during the supersonic expansion. The velocity distribution of the DEE beam was determined by TOF measurements to have a peak velocity of 1120 m/sec and a full width at half maximum of 30 percent. The beam was collimated by a skimmer and, after passing through two pressure reducing differential pumping chambers, it was crossed by the laser beam. The molecular beam was defined to an angular divergence of ~1.6°.

The infrared photons were produced by a Gentec DD-250 CO_2 TEA laser tuned to the P(24) line in the 001-020 vibrational band at 1043.16 cm^{-1}. The TT conformer of DEE has an absorption band at 1047 cm^{-1} and the less stable (by 1.1 kcal/mole) TG conformer absorbs at 1021 and 1067 cm^{-1}. A photon drag detector was used to measure the temporal output of the laser pulse; the intensity is strongest near the beginning of the pulse, which has a 300 nsec FWHM and a long tail extending to 0.6 μsec with an average intensity of ~40 percent of the peak. The laser was run at a 50 Hz repetition rate. For all the TOF data but the m/e = 26 TOF, the total energy fluence crossing the molecular beam in the interaction region is estimated to be ~2.4 J/cm^2. The m/e = 26 TOF was taken at an energy

fluence of ~1.8 J/cm^2. The laser light was unpolarized and was focussed onto the molecular beam with a 10" focal length spherical zinc selenide lens. For the total signal dependence on laser fluence, the lens position was kept fixed and the fluence was adjusted from 5.5 to 0.5 J/cm^2 by attenuating the laser beam on passing it through a gas cell filled with from 0 to 360 torr of C_2H_4.

The dissociation products were detected in the plane of the laser and molecular beam by a rotatable ultra-high vacuum mass spectrometer consisting of an electron bombardment ionizer, quadrupole mass filter, and particle counter. The emission current in the ionizer was 10 mA with a 240 eV electron energy. The flight path between the beam crossing point and the ionizer was 20.7 cm. TOF distributions were measured in the usual way.[12]

Signal was observed when the quadrupole mass spectrometer was set to pass the following mass to charge ratios: m/e = 14, 15, 26, 27, 28, 29, 30, 31 and 44; after very long counting times a very small signal was detected at m/e = 57. These masses correspond to CH_2^+, CH_3^+, $C_2H_2^+$, $C_2H_3^+$, (CO^+, $C_2H_4^+$), ($C_2H_5^+$, CHO^+), (CH_2O^+, $CHOH^+$), (CH_2OH^+, CH_3O^+), $C_2H_4O^+$ and $C_2H_5O^+$ and to $C_2H_4OCH^+$. No measurable signal was detected at m/e = 46, 58, or 59 corresponding to $C_2H_5OH^+$, $C_2H_4OCH_2^+$ and $C_2H_5OCH_2^+$ or their conformers after signal averaging for 300,000 laser shots for each. Typical signal levels at a detection angle of 10° from the molecular beam and a photon fluence of ~2.4 J/cm^2 ranged from 0.14 to 0.82 counts/laser pulse for all but m/e = 57, at which the signal level was 0.003 counts/laser pulse. A good signal to noise ratio was obtained for all masses but 14, 15 and 57.

RESULTS AND ANALYSIS

A. Identification of the Molecular Elimination Channel

The m/e = 31 (CH_2OH^+, CH_3O^+) TOF measured at an angle of 10° to the molecular beam is shown in Fig. 2. Let us first focus our attention on the faster peak in this spectrum. This sharp spectrum, which corresponds to a narrow energy distribution at a relatively high average translational energy, can only contain contributions from the heavier molecule of each pair of products shown in Fig. 1. It is easily calculated from momentum conservation in the center of mass coordinate system and velocity vector addition that about 24 kcal/mole of the total available energy would have had to be released as translational energy of the products for the acetaldehyde, ethanol or ethoxy radical product to arrive at the detector at times corresponding to the peak of the fast distribution in the m/e = 31 TOF. The total product translational energy would have to be as much as ~115 kcal/mole in the peak of the distribution if the $C_2H_5OCH_2$ product were to give the fast peak in the m/e = 31 TOF spectrum. Thus, it is very clear that the fast velocity product in the mass 31 TOF must be due to one of the two energetically allowed molecular elimination reactions as only these two channels have enough available energy through the conversion of exit potential energy barrier to give the observed product translational energies. The radical channels from simple bond rupture are not expected to have such a high average translational energy release with such a narrow energy distribution, even if an excessively large number of photons are absorbed before dissociation.

Identification of the molecular elimination channel would be easy if we had observed the same fast product velocity distribution at m/e = 46, ($C_2H_5OH^+$), but the fast product was not observed at this mass or at m/e = 44 (CH_3CHO^+, CH_2CHOH^+). This is understandable because the energies required to dissociate $C_2H_5OH^+$ or CH_3CHO^+ to their smaller ion fragments are known to be small, ~15 kcal/mole, and the ionization of highly vibrationally excited C_2H_5OH or CH_3CHO products is not expected to yield the parent ion in electron bombardment ionization. By careful examination of the masses at which daughter ions of the heavy product appear and of the masses at which daughter ions of the lighter partner C_2H_4 for the ethanol product or C_2H_6 for the acetaldehyde product appear one can be reasonably certain that DEE dissociates to form ethanol and ethylene but not acetaldehyde and ethane. First, m/e = 31 is the major ion mass fragment of ethanol[13]. Second, no signal from acetaldehyde was detected at m/e = 31 in a previous IRMPD experiment on the same apparatus in which acetaldehyde was a product;[2] an H atom migration must occur to get signal from acetaldehyde at m/e = 31 CH_2OH^+. Third and perhaps most important, the lighter fragment of the molecular elimination channel does not appear in the m/e = 30 or 29 TOF spectra (see Fig. 3 and Fig. 4) but it does appear in the m/e = 28 spectra. If the C_2H_6 product were being formed one would expect it to give m/e = 30 or 29, yet there is no additional broadening of the fast peak in the m/e = 30 or 29 TOF which is expected from the lighter fragment. The lighter, faster product is not detected until the m/e is tuned to 28 ($C_2H_4^+$), as would be expected if DEE dissociates to give ethanol and ethylene. The TOF of m/e = 28 is shown in Fig. 5.

B. Identification of the Radical Channel

The TOF spectra of m/e = 44 ($C_2H_4O^+$) at 10° from the molecular beam is shown in Fig. 6. The fast partner to this velocity distribution appears in the TOF spectra taken at masses m/e = 29, 28, 27 (Fig. 7), 26 (Fig. 8), 15 and 14. Thus the radical channel, reaction (1) which forms $C_2H_5O + C_2H_5$ must be occurring since the CH_3 product in the other radical channel cannot give any contribution at the higher of masses. The extremely small signal at m/e = 57 (0.003 counts/laser puls suggests that a very small fraction (certainly < 1 percent) of the DEE r ssociate by breaking a C-C bond:

$$C_2H_5OC_2H_5 \rightarrow C_2H_5OCH_2 + CH_3 \qquad (3)$$

However the signal at mass 57 is so small that the dissociation from dimers, $(C_2H_5OC_2H_5)_2$, cannot be ruled out as the possible source. The dissociation of DEE into two channels with vastly different translational energy distributions can also be seen easily in Fig. 8 as this TOF has contributions from both of the molecular elimination products and the lighter radical product. The momentum-matched heavier radical product and the heavier molecular product can be seen in Figs. 2 and 3 without contributions from the overlapping lighter product.

C. Product Translational Energy Distributions:

1. $C_2H_5OC_2H_5 \rightarrow C_2H_5O + C_2H_5$

When a molecule dissociates to two fragments, the linear momentum of one fragment is equal in magnitude and opposite in direction to that of the other fragment in the center of mass coordinate system, so the measured velocity distribution of one derived from the experimental measurements will completely define the velocity distribution of the other fragment and the total center of mass translational energy distribution P(E') of the dissociation process. The TOF distribution of the C_2H_5O product (Fig. 6) was fit by a trial and error forward convolution method using a completely flexible point form P(E'). The good fit shown in dotted line in Fig. 6 was calculated from the P(E') in Fig. 9. We used this P(E') to fit the slow peak in the m/e = 26 and 27 TOF spectra (Figs. 8 and 7) by varying the relative amounts of C_2H_5O and C_2H_5 product contributing to these TOF distributions. In both cases the best fit was obtained when only the C_2H_5 product's contribution was used.

During the trial and error fitting procedure of the m/e = 44 TOF, the daughter ions of the C_2H_5O product, it was found immediately that the better fits were achieved by making the P(E') peak at translational energies near 0 kcal/mole. We then tried to fit the data with a translational energy distribution derived with RRKM theory. In an IRMPD experiment the molecules dissociate from a distribution of levels above the dissociation limit determined by the experimental conditions. Thus the RRKM translational energy distribution used to fit the data should be a sum of the translational energy distributions from single energy levels weighted by the

fraction of molecules that dissociate from each level. In order to estimate weighting factors for these levels, we simulated the infrared photon absorption and dissociation process for this system with a simple rate equation model described in detail elsewhere.[14] We calculated the RRKM dissociation rate constants (see Fig. 10) from published molecular vibrational frequencies and frequencies of transition states chosen to reproduce the estimated A-factor and activation energies of Benson and O'Neal for the radical channel and the reported parameters of Istvan and Peter for the molecular elimination channel (at 800°K). This procedure is known to give reasonable RRKM rate constants as a function of internal energy.[15] The spread of dissociating energy levels was found to be only weakly dependent on the parameters of the model which are not known, most importantly, the change in photon absorption and stimulated emission cross section as a function of internal energy. The simulation suggested a representative form for the relative dissociation yields from a group of neighboring energy levels which we used to calculate the effective RRKM P(E'). With each level spaced 2.983 kcal/mole apart, corresponding to the photon energy, the contribution from neighboring energy levels to the RRKM translational energy distribution were weighted by factors of 8, 20, 38, 60, 73, 80, 73, 60, 38, 20, 8[16]; this dissociating population distribution was used to calculate the RRKM P(E') at several median dissociation energies. The data was then fit with the resulting P(E') for each mean energy. The model calculation that gave this shape distribution accounted for the fact that we only detect dissociation occurring before the excited molecule moves out of the viewing region of the detector. It includes the competition of

dissociation to molecular as well as radical products with photon absorption above the dissociation limits. The unknown parameters in the model which relate to the absorption and stimulated emission of photons had a large effect on the actual median energy level from which dissociation occurred, but, as will be seen, the product velocity distribution from the radical channel helped limit the uncertainty in this energy level.

We then attempted to fit the m/e = 44 TOF with several different averaged RRKM translational energy distributions. The best fit was achieved with molecules dissociating from the eleven energy levels 1.73, 4.71, 7.69, 10.68, 13.66, 16.64, 19.63, 22.61, 25.59. 28.57 and 31.56 kcal/mole above the 81.8 kcal/mole dissociation limit. The translational energy distributions, calculated using RRKM theory, from each of these levels was weighted by the population distribution above and summed to give the P(E') used to fit the data. We will call this the "averaged 16.64 kcal/mole P(E')." This is the P(E') shown in Fig. 9. It is slightly broader than the usual single level RRKM translational energy distribution calculated assuming all the molecules dissociate from the level 16.64 kcal/mole above the dissociation limit. Acceptable fits to the TOF data could also be obtained with an "averaged" 22.61 kcal/mole P(E') and an averaged 10.68 kcal/mole P(E'), but not from dissociating levels peaked at higher or lower energies than these. Thus the measured C_2H_5O TOF suggests that most of the detected radical products were formed from DEE dissociating from energy levels between 5 and 28 kcal/mole above the 81.8 kcal/mole dissociation limit (including energy levels in the population distribution weighted by a factor of 60 or greater). It should be noted that since the excited diethyl

ether molecule is travelling ~11.2 x 10^4 cm/sec through a small region (~3 mm long) viewed by the detector, we are mainly sensitive to molecules with dissociation times shorter than a few microseconds. Using the calculated RRKM dissociation rate constant of 0.5641 x 10^4 sec^{-1}, only about 1 percent of the DEE that dissociates to radical products at 16.64 kcal/mole above the dissociation limit will dissociate within the detector viewing volume and have a chance to be detected.

2. $C_2H_5OC_2H_5 \rightarrow C_2H_5OH + C_2H_4$

The fast peak in the m/e = 31 TOF (Fig. 2) was fit with a completely flexible point form P(E'). The fit shown in dotted line in Fig. 2 was calculated from the P(E') shown in Fig. 11. The P(E') peaks at ~26 kcal/mole in translation and extends out to beyond 45 kcal/mole translational energy, with an average energy released of ~24 kcal/mole. The fits shown for the fast peaks in the m/e = 26 and 27 TOF's (Figs. 8 and 7) were calculated from this P(E') using the relative contribution of the C_2H_5OH and C_2H_4 to these masses as the only variable parameter.

Assuming (1) the A-factor and activation energy of Istvan and Peter for this channel are correct and (2) the conclusions about the energy levels those molecules which dissociated to radicals had reached are also correct, we can estimate the energy levels from which the molecules dissociated to ethanol and ethylene. Since the RRKM rate constants for the molecular elimination channel are higher than those for the radical channel for internal energies up to ~125 kcal/mole (see Fig. 10), the molecular eliminations will occur on the average from slightly lower energy levels.

How much lower will depend on the mean energy level from which the radical dissociations occur and the fraction of molecules that dissociate during the laser pulse. A good estimate based on our approximate modeling is that the molecules that dissociate via rxn. (2) and are detected do so from energy levels that are 1-9 kcal/mole below the energy levels from which the radical products are formed. We thus estimate that the majority of molecular eliminations occur from energy levels 0-25 kcal/mole above the radical dissociation limit of 81.6 kcal/mole; i.e. DEE dissociates to give molecular products from energy levels mostly between 82 and 107 kcal/mole above its zero point level.

D. Branching Ratio and Total Product Yield Dependence on Laser Power

The integrated TOF signal at m/e = 26 as a function of laser power is shown in Fig. 12. In spite of the large error bars, one can see the signal still increased with laser power at the higher powers used in this experiment. Quantitative interpretation of this data is, however, quite difficult in this case. There are two dominant factors which would cause our signal level to rise in this measurement. The first is simply that more molecules absorb enough photons during the laser pulse to reach energy levels above one or both dissociation limits. The second factor arises from our experimental arrangement. An excited DEE molecule will spend at most 2.7 μsec in the viewing region of the detector. Because the lifetimes for dissociation to molecular or radical products at an energy level of 98 kcal/mole above the ground state are ~13 and ~180 μsec respectively, we

detect only a small fraction of the total number of dissociations. With increasing laser power, the average energy level a molecule will reach above the dissociation limit increases. At the higher excitation levels, the dissociation rate constants become higher and a greater fraction of the molecules will dissociate within the region viewed by the detector. Even when most of the molecules are already above the dissociation limit and no increase in the number of molecules above the dissociation limit is expected, higher laser intensity will still give a larger signal. For instance, the fraction of dissociations forming radical products that occur within the viewing region of the detector increases by a factor of 3, from ~1 percent to ~3 percent, if the molecules dissociate from an energy level 19.63 kcal/mole compared to 16.64 kcal/mole above the dissociation limit.

A crude determination of a branching ratio between these two channels was made by comparing the total signal at m/e = 14, 15, 26, 27, 28, and 29 ascribed to C_2H_5 with the total signal at all the masses counted ascribed to C_2H_5OH. If the branching ratio were 1:1, and the ionization cross sections are the same we would expect the total ion signal from C_2H_5 to be 10.8 times that of C_2H_5OH due to the differences in laboratory angular and velocity distribution of these two products. The observed total ion signal for C_2H_5 is 3 times that for C_2H_5OH, giving a branching ratio of 78 percent molecular channel and 22 percent radical channel. A similar analysis of the total ion signals of C_2H_5 compared to C_2H_4 gives a branching ratio of 76 percent : 24 percent. However, the ion signal of C_2H_5O compared to C_2H_5OH gives a branching ratio of 95 percent : 5 percent. Our lack of data at m/e = 45 may be the

source of the discrepancy, but as this would only shift the branching ratio in favor of the molecular channel in the comparison of the C_2H_5 and C_2H_5OH counts and would not affect the C_2H_4:C_2H_5 ratio, we may arrive at a lower bound of ~70 percent molecular channel (2). The branching ratio predicted from the rate parameters is critically dependent on the mean energy level from which the molecules dissociate for each channel. In a calculation where the molecular products are formed from energies peaked at 107 kcal/mole above the ground state of DEE and the radical products are from 3 kcal/mole higher energies, the branching ratio is 85.3 percent and 14.7 percent in qualitative agreement with our crude estimate.[17] Our best estimate of the energy levels from which dissociation occurred based on the m/e = 44 translational energy distribution was lower in energy by ~9 kcal/mole; at these lower energies the radical channel would be <5 percent of the dissociation yield.

IV. DISCUSSION

The effect that an exit channel barrier has on the asymptotic translational energy distribution of the products has been treated theoretically by Marcus[18] and Hase et al.[19] Hase et al.[19] studied ethyl radical decomposition to H + C_2H_4 with Monte Carlo classical trajectories on potential energy surfaces with different exit channel barrier heights. The exit channel barrier results from the C-C single bond in the reactant shortening to a C=C double bond in the ethylene product. He found that the shape of the product translational enegy distribution at the top of the barrier agreed with the predictions of RRKM theory, but that the distribution broadened and shifted to higher translational energies as the reaction was allowed to proceed beyond the top of the exit channel barrier. The effect was larger for a 3.5 kcal/mole barrier than it was for a 0.1 kcal/mole barrier. Marcus[18] demonstrated the application of RRKM theory to prediction of final product translational energy distributions when the reaction proceeds through a tight transition complex which involves an exit channel barrier. He showed that one should allow for the evolution of the RRKM transition state as the reaction proceeds down the exit channel barrier. In his example case, the bending vibrations excited in the tight transition state are coupled into translation and rotation of the products as they recoil from each other.

The concerted reaction forming ethanol and ethylene has a large exit barrier estimated at ~50 kcal/mole. The measured product translational energy distribution shown in Fig. 11 peaks at ~24 kcal/mole translational energy. At an RRKM critical configuration calculated from the Istvan and

Peter A-factor and activation energy only 1.5 to 2.5 kcal/mole is in the relative motion of the products, if the molecule dissociates from energies averaging around 14, and 39 kcal/mole respectively above the dissociation limit, so one might conclude that the interactions between the products as they descend the exit barrier considerably alters their energy distribution at the top of the barrier. Their final translational energy is measured to be almost 1/2 of the exit barrier height.

The fraction of the exit channel barrier energy released to translation in this four center elimination reaction is significantly higher than that measured for the four center HCl elimination from halogenated hydrocarbons by Suzbo et al.,[3] but considerably smaller than the 70 percent released to translation in the IRMPD dissociation of ethyl vinyl ether to CH_3CHO + C_2H_4.[2] The latter comparison is particularly interesting as both involve hydrogen atom transfer and breaking of a C-O bond, as here both bonding electrons move away from the CO bond in a concerted reaction, the C-O interaction becomes repulsive , and the translational energy of the product molecules is mainly due to the repulsive energy release of this interaction. Although the fractions of the exit barriers appearing in translational energy are somewhat different for EVE and DEE, they have a similar average translational energy release, 31 and 26 kcal/mole respectively. In concerted reactions with large exit barriers, the structure of the transition state will determine the energy partitioning to a large extent. If the chemical bonds in the products which are to be formed are extensively stretched in the transition state, significant vibrational excitation is expected. On the other hand the longer the bond

which is to be broken is extended, the less important the repulsive energy release will be. In the four center HCl elimination reactions, the C-Cl bond to be broken must be significantly extended, but in EVE or DEE, in view of the enormous translational energy release it is likely that the C-O bonds to be broken are not significantly extended when the interaction suddenly becomes repulsive.

The shape of product translational energy distribution (Fig. 9) for the radical channel (1) was in agreement with RRKM theory for reactions proceeding through a loose transition state. We accounted for the fact that in an IRMPD experiment, the reactant molecules dissociate from a distribution of energy levels above the dissociation limit by using an averaged RRKM P(E') to fit the data. The exact form of this distribution was described in Part III C. The best fit P(E') was calculated with molecules dissociating to radicals from a spread of energy levels peaked at 16.64 kcal/mole above the dissociation limit. The average energy released to translation of the radical products detected was 1.6 kcal/mole.

Because the photon absorption and stimulated emission cross sections as a function of energy for a highly energized molecule are not generally known, one is usually uncertain in an IRMPD experiment as to what mean energy level the absorbing molecule will reach before it dissociates. An attempt was made in this study to reduce this uncertainty considerably. Assuming (1) that the thermochemical A-factor and activation energy reported for the dissociation channel are correct and (2) that the translational energy distribution of the products is correctly predicted by RRKM theory, one can determine the approximate mean energy level from which the molecule

dissociated to radicals by attempting to fit the data with various predicted RRKM P(E')'s. The mean total available energy for the RRKM P(E') that fit the measured velocity distribution determines the mean energy level from which the molecules dissociated. The method is only weakly dependent on the assumed shape of the distribution of energies of the dissociating levels. If the radical product TOF were measured carefully at several laser fluences, one might expect also to gain some information on how the mean energy of the dissociating levels increases with photon intensity.

It should be noted that if the endoergicity of the C-C bond fission channel $CH_3CH_2OCH_2CH_3 \rightarrow CH_3CH_2OCH_2 + CH_3$ (3) were ~85 kcal/mole, similar to the radical channel (1), we would have seen evidence for this channel. Since the $\log_{10}A$ for this simple bond fission should be ~16 and no exit barrier is expected, only a larger dissociation energy than 85 kcal/mole would explain why channel (3) was not competitive with the radical channel (1).

ACKNOWLEDGMENT

This work was supported by the Office of Naval Research under Contract Number N00014-75-C-0671.

REFERENCES

1. Aa. S. Sudbo, P. A. Schulz, E. R. Grant, Y. R. Shen and Y. T. Lee, J. Chem. Phys. 70, 912 (1979).

2. F. Huisken, D. Krajnovich, Z. Zhang, Y. R. Shen and Y. T. Lee, J. Phys. Chem. 78, 3806 (1983).

3. Aa. S. Sudbo, P. A. Schulz, Y. R. Shen and Y. T. Lee, J. Chem. Phys. 69, 2312 (1978).

4. D. Krajnovich, F. Huisken, Z. Zhang, Y. R. Shen and Y. T. Lee, J. Chem. Phys. 77, 5977 (1982).

5. C. R. Quick, Jr. and C. Wittig, J. Chem. Phys. 72, 1694 (1980).

6. D. S. King and J. C. Stephenson, Chem. Phys. Lett. 51, 48 (1977); J. C. Stephenson and D. S. King, J. Chem. Phys. 69, 2485 (1978).

7. K. J. Laidler and D. J. McKenney, Proc. Roy. Soc. 278A, 517 (1964).

8. S. Istvan and H. Peter, Mag. Kem. Foly. 81, 120 (1975).

9. S. W. Benson and H. E. O'Neal, Kinetic Data in Gas Phase Unimolecular Reactions, NSRDS-NBS 21 (1970).

10. Y. T. Lee, J. D. McDonald, P. R. LeBreton and D. R. Herschbach, Rev. Sci. Instrum. 40, 1402 (1969).

11. H. Wieser, W. G. Laidlaw, P. J. Krueger and H. Fuhrer, Spectrochim. Acta 24A, 1055 (1967).

12. See, for example, ref. 3.

13. E. Stenhagen, S. Abrahamsson and F. W. McLaffery ed., Atlas of Mass Spectral Data (John Wiley and Sons, New York) 1969.

14. P. A. Schulz, Ph.D. thesis, University of California (1979).

15. P. J. Robinson and K. A. Holbrook, Unimoleclar Reactions (Wiley, New York) 1972.

16. Or if all these levels are not above the dissociation limit, as for the case when 10.68 kcal above the dissociation limit, we used a narrower distribution: 8, 20, 60, 80, 60, 20, 8.

17. For this calculation, the spread of energy levels from which dissociation in the viewing region of our detector occurred was comparable to that described in Part 3C. We used a ground state photon absorption cross section of 1×10^{-18} cm^2 which fell exponentially to 3.2×10^{-19} at the radical dissociation limit. The excitation level described was reached at a photon fluence of 1.83 J/cm^2; this was the average excitation of the molecules that dissociated in the collision region. The average excitation of all the molecules at the end of the laser pulse was ~80 kcal/mole. These parameters predicted a larger increase in signal with increasing laser power than our data showed.

18. R. A. Marcus, J. Chem. Phys. 62, 1372 (1975).

19. W. L. Hase, R. J. Wolf and C. S. Sloane, J. Chem. Phys. 71, 1911 (1979).

FIGURE CAPTIONS

Fig. 1. The low energy dissociation channels of $C_2H_5OC_2H_5$. ΔH^o_{300} values were calculated from values tabulated in Rosenstock et al., J. Phys. Chem. Ref. Data 6, Supp. 1, (1977) for the ethanol and acetaldehyde channels and estimated to be 85 kcal/mole for the $C_2H_5OCH_2$ channel using group additivity rules (S. W. Benson, Thermochemical Kinetics, Wiley Interscience, New York, 1976) and the heat of formation of CH_3OCH_2. The energetics of the $C_2H_5O + C_2H_5$ radical channel are those of Ref. 9. The barrier in the ethanol channel, 66 kcal/mole from the reactant, was reported in Ref. 8.

Fig. 2. TOF distribution of m/e = 31, (CH_2O^+, $CHOH^+$) at 10° from the molecular beam. • Experimental points, ——— best fit, obtained by adding the individual contributions of C_2H_5OH (——— • ———) and C_2H_5O (—— —— ——). The C_2H_5OH contribution was calculated using the P(E') in Fig. 11. The C_2H_5O contribution was calculated using the P(E') in Fig. 9. The relative intensities were varied to obtain the best fit and an isotropic center of mass angular distribution was used. Pnoton energy fluence = 2.4 J/cm^2.

Fig. 3. TOF distribution of m/e = 30, (CH_2O^+, $HCOH^+$) at 10° from the molecular beam. • Experimental points, ——— best fit, obtained by adding the individual contributions of C_2H_5OH (——— • ———) and C_2H_5O (—— —— ——). The individual contributions were calculated as in Fig. 2. Photon energy fluence = 2.4 J/cm^2.

Fig. 4. TOF distribution of m/e = 29 ($C_2H_5^+$, COH^+), at 10° from the molecular beam. Data is shown with a 5 point polynomial smooth. • Experimental points, ———— best fit, obtained by adding the individual contributions of C_2H_5OH (—— • ——) and C_2H_5 (—— — ——). The C_2H_5OH contribution was calculted as in Fig. 2. The C_2H_5 contribution was calculated from the P(E') shown in 9 which is derived from the C_2H_5O TOF distribution (Fig. 6). Photon energy fluence = 2.4 J/cm^2.

Fig. 5. TOF distribution of m/e = 28, (CO^+, $C_2H_4^+$), at 10° from the molecular beam. • Experimental points, ———— best fit obtained by adding the individual contributions of C_2H_4 (—— • • ——), C_2H_5OH (—— • ——) and C_2H_5 (—— — ——). The shape of each individual TOF distribution is fixed by the P(E') that fit the m/e = 44 and 31 TOF's (Fig. 6 and 2). The relative intensity of each contribution was varied to obtain best fit.

Fig. 6. TOF distribution of m/e = 44, $C_2H_4O^+$, at 10° from the molecular beam. • Experimental points, ———— fit calculated using the P(E') in Fig. 9 and an isotropic center of mass angular distribution. Photon energy fluence = 2.4 J/cm^2.

Fig. 7. TOF distribution of m/e 27, $C_2H_3^+$, at 10° from the molecular beam. • Experimental points. ———— best fit obtained by adding the individual contributions of C_2H_4, C_2H_5OH and C_2H_5 as in Fig. 7. Photon energy fluence = 2.4 J/cm^2.

Fig. 8. TOF distribution of m/e = 26, $C_2H_2^+$, at 10° from the molecular beam. • Experimental points. ———— best fit obtaining by adding the individual contributions of C_2H_4 (—— • • ——), C_2H_5OH (—— • ——) and C_2H_5 (—— — ——). The shape of each individual TOF distribution is fixed by the P(E') that fit the m/e = 44 and 31 TOF's (Fig. 6 and 2). The relative intensity of each contribution was varied to obtain best fit. Photon energy fluence = 1.8 J/cm^2.

Fig. 9. Center-of-mass translational energy distribution for the radical dissociation channel DEE → C_2H_5O + C_2H_5 derived from the m/e = 44, $C_2H_4O^+$, TOF distribution (Fig. 6). This P(E') was used to obtain the calculated fits shown in all other TOF distributions which contained contributions from C_2H_5O or C_2H_5.

Fig. 10. RRKM rate constant curves for DEE decomposition assuming E_a = 66 kcal/mole and $\log_{10}A$ = 13.9 for the reaction producing C_2H_5OH + C_2H_4 and E_a = 81.8 and $\log_{10}A$ = 16.3 for the reaction producing C_2H_5O + C_2H_5.

Fig. 11. Center-of-mass translational energy distribution for the molecular elimination channel DEE → C_2H_5OH + C_2H_4 derived from the ethanol contribution to the m/e = 31 TOF distribution (Fig. 2). This P(E') was used to obtain the calculated fits shown in all other TOF distributions which contained contributions from C_2H_5OH or C_2H_4.

Fig. 12. Integrated signal at m/e = 26 as a function of photon energy fluence. • Experimental points. Error bars represent plus or minus one standard deviation of the statistical error. The laser pulse shape is constant, so intensity increased with fluence.

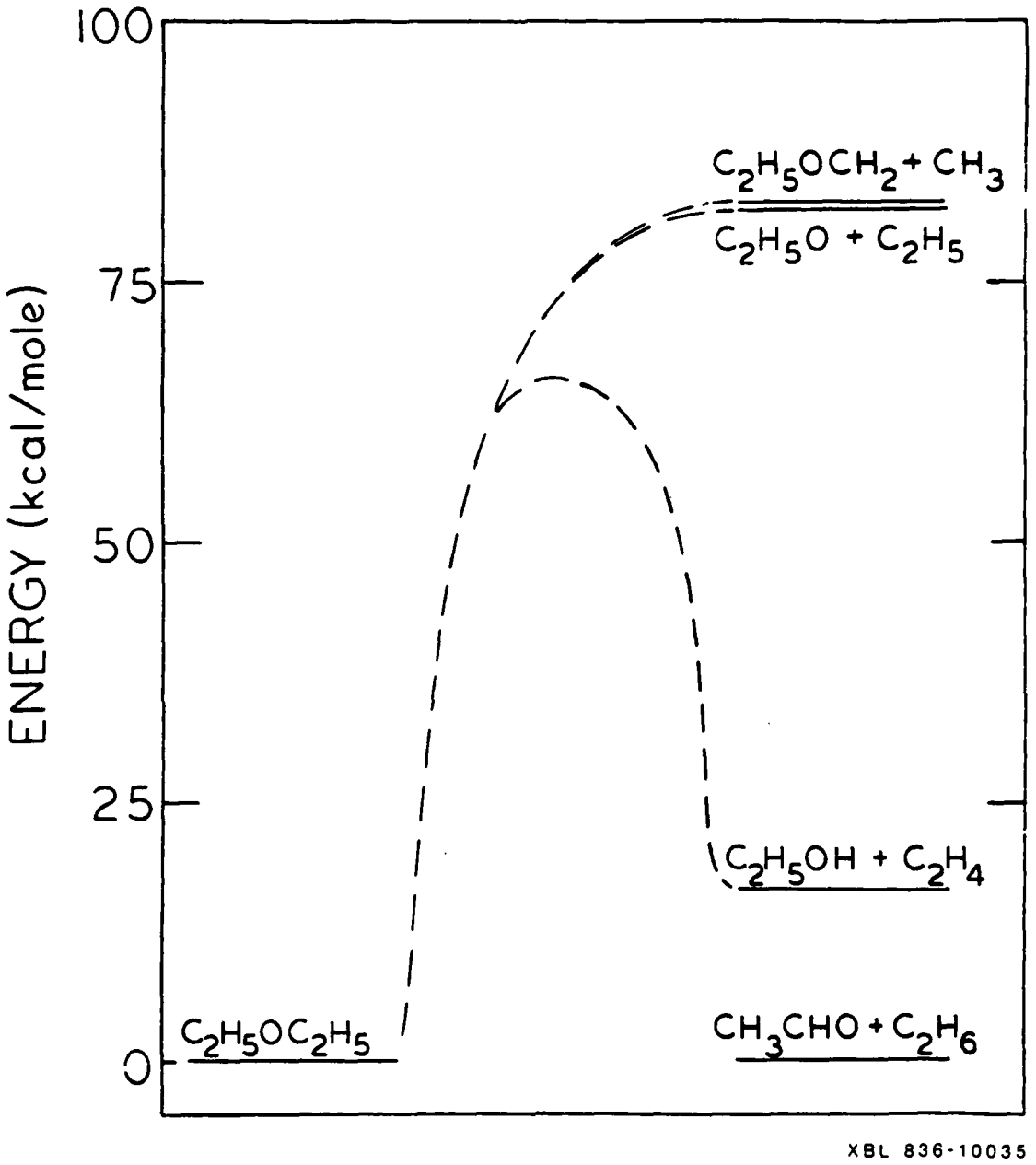
100
75
50
25
0
ENERGY (kcal/mole)
$C_2H_5OCH_2 + CH_3$
$C_2H_5O + C_2H_5$
$C_2H_5OH + C_2H_4$
$C_2H_5OC_2H_5$
$CH_3CHO + C_2H_6$
XBL 836-10035

Fig. 1

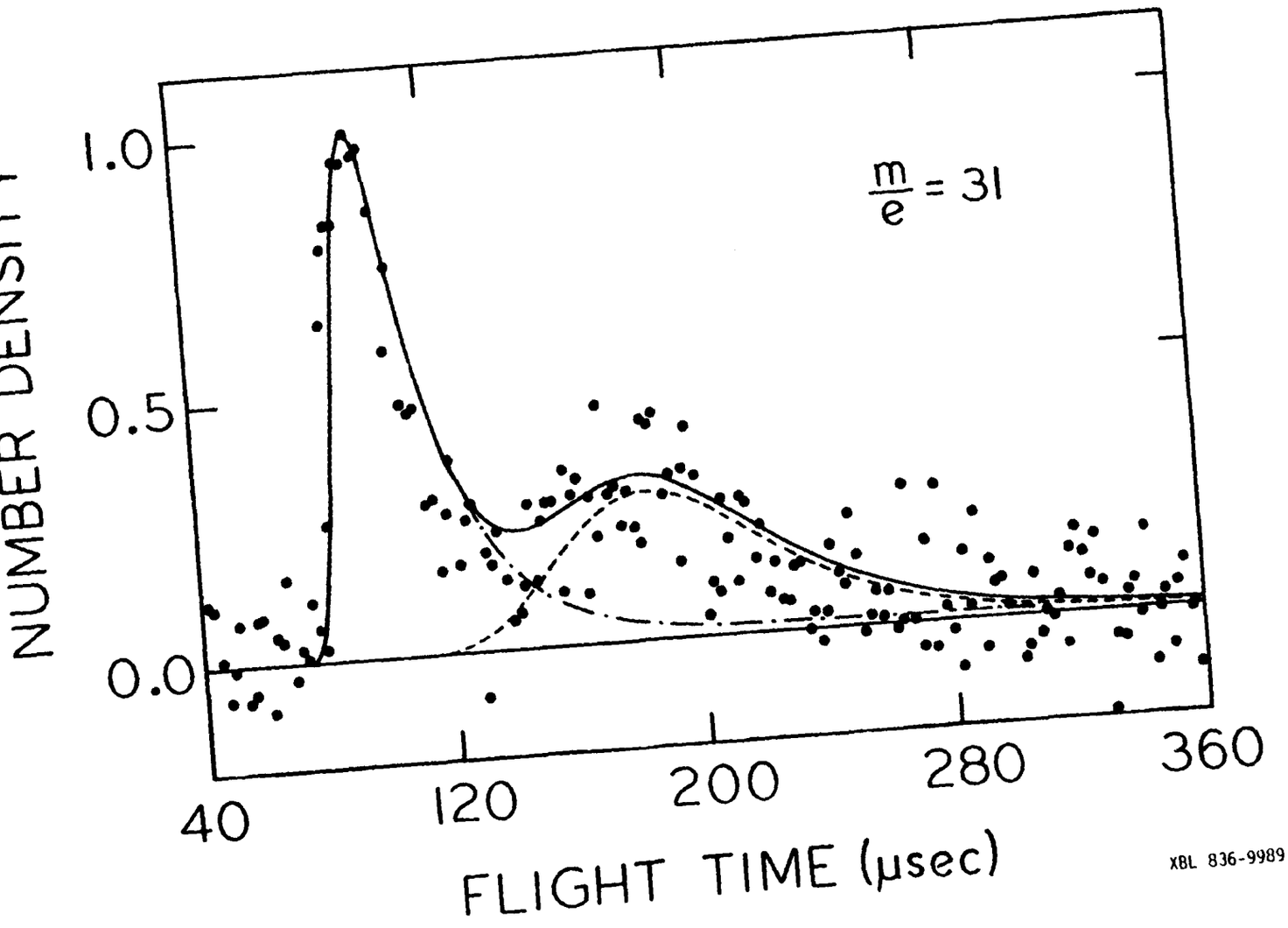
NUMBER DENSITY
1.0
0.5
0.0
m/e = 31
40
120
200
280
360
FLIGHT TIME (μsec)
XBL 836-9989

Fig. 2

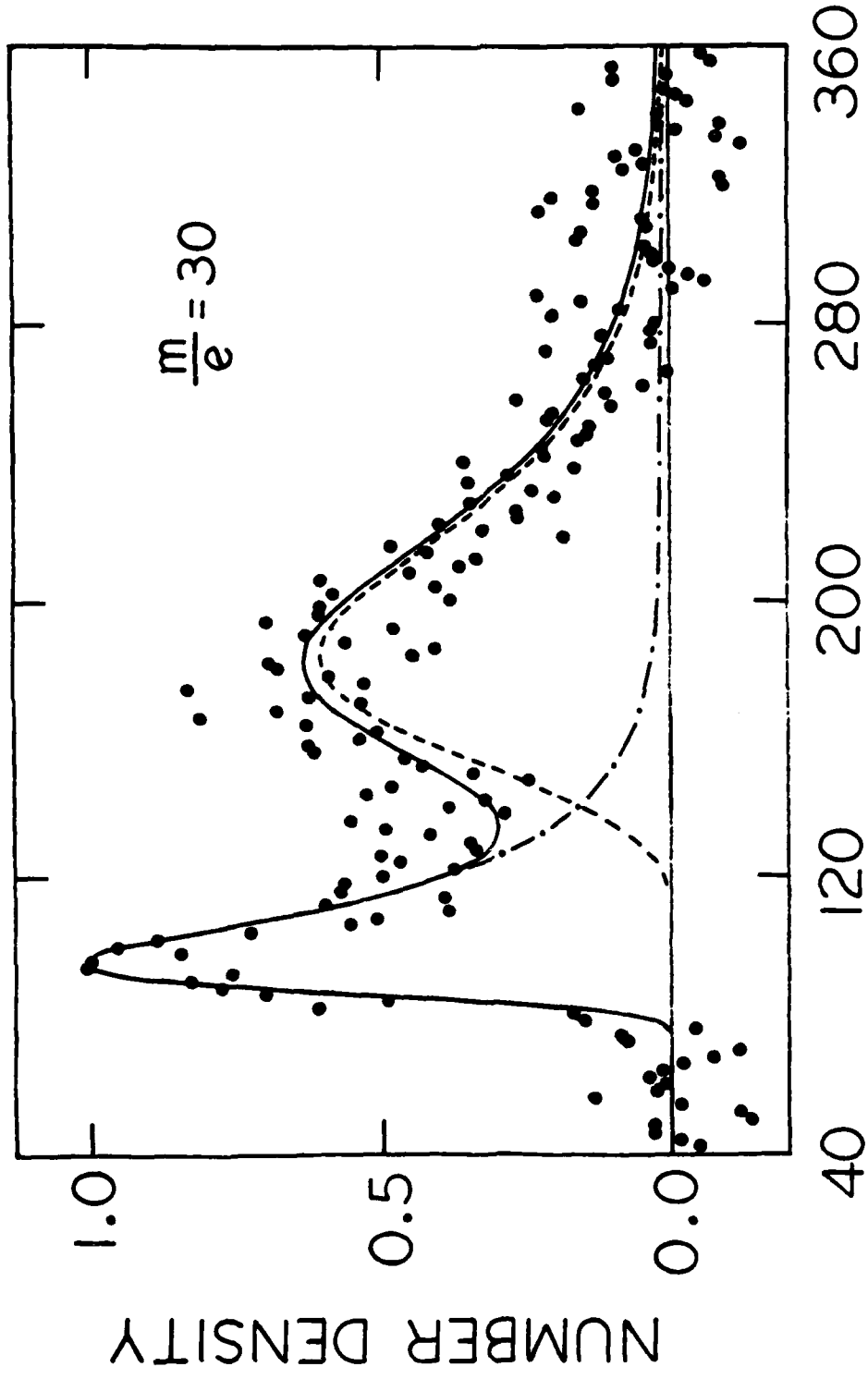

XBL 836-9991

Fig. 3

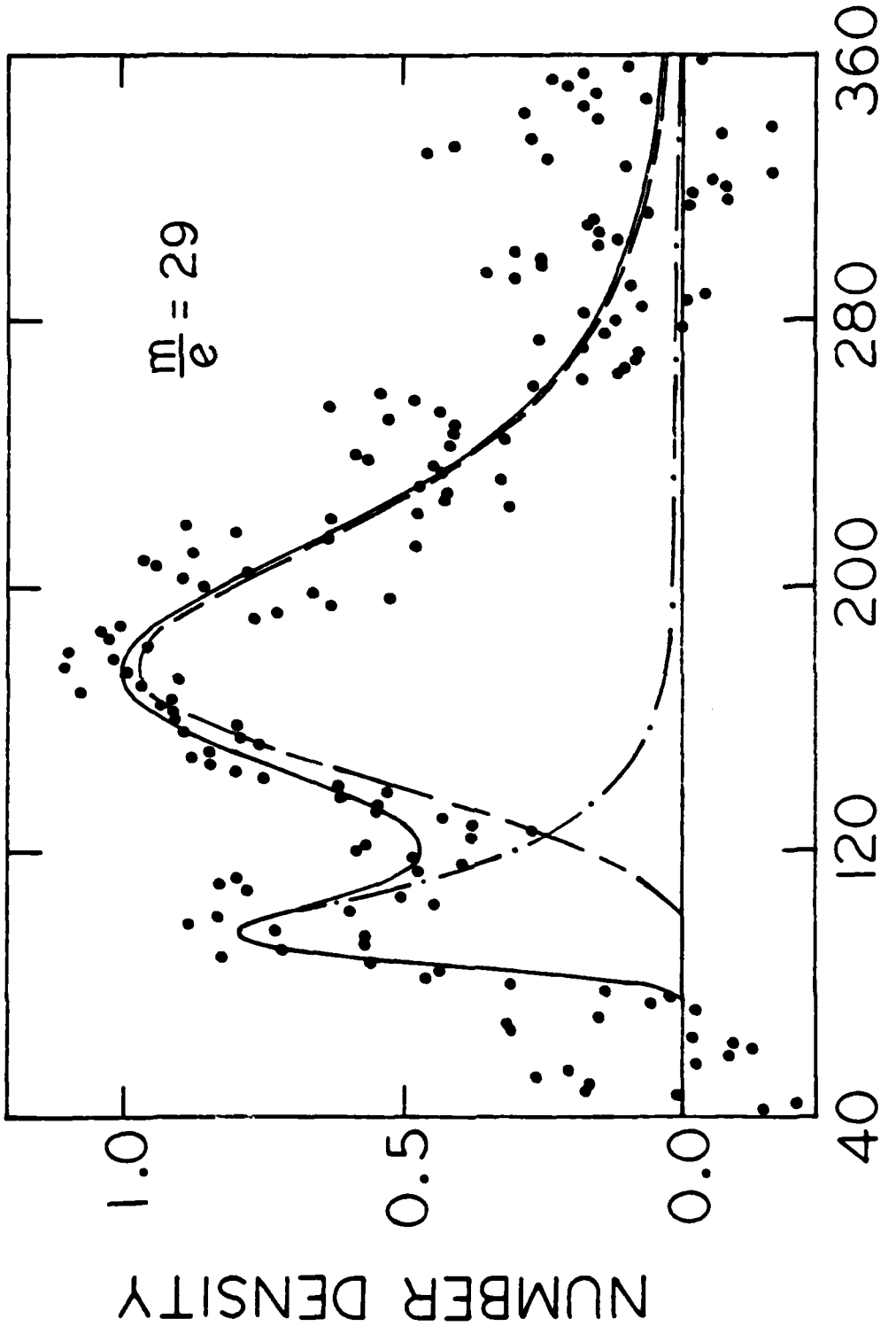

XBL 836-9988

Fig. 4

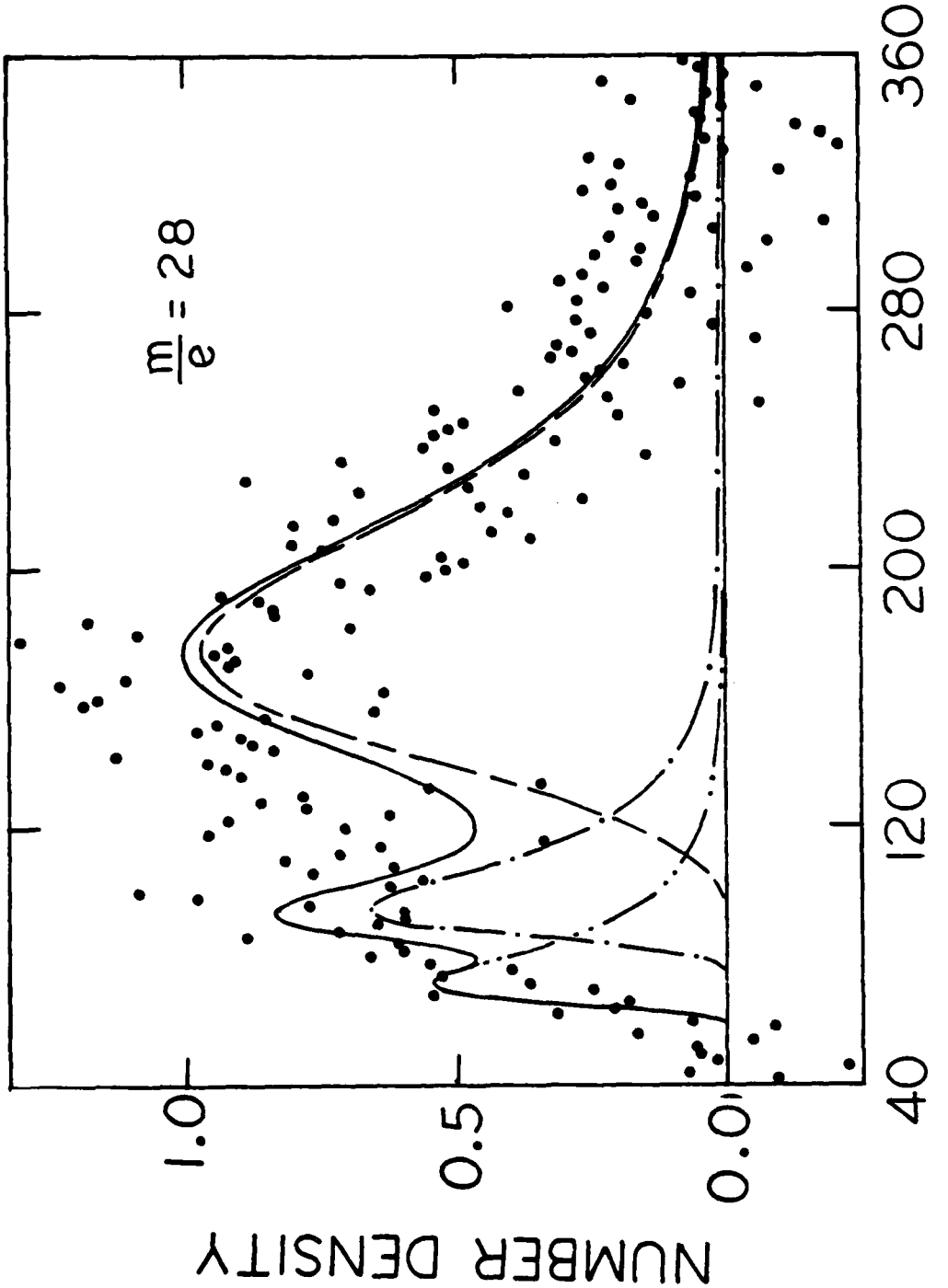

XBL 836-9986

Fig. 5

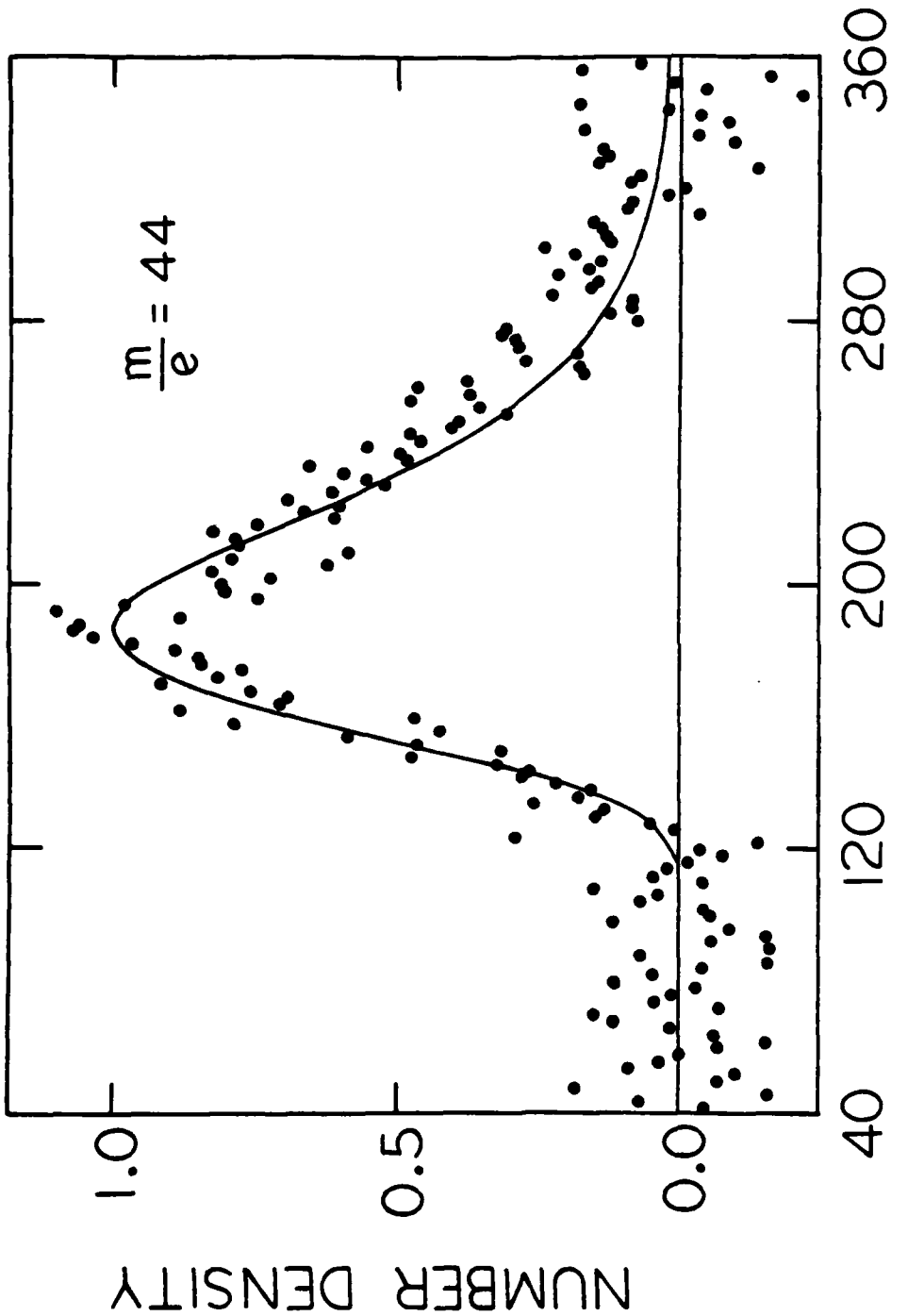

XBL 836-10034

Fig. 6

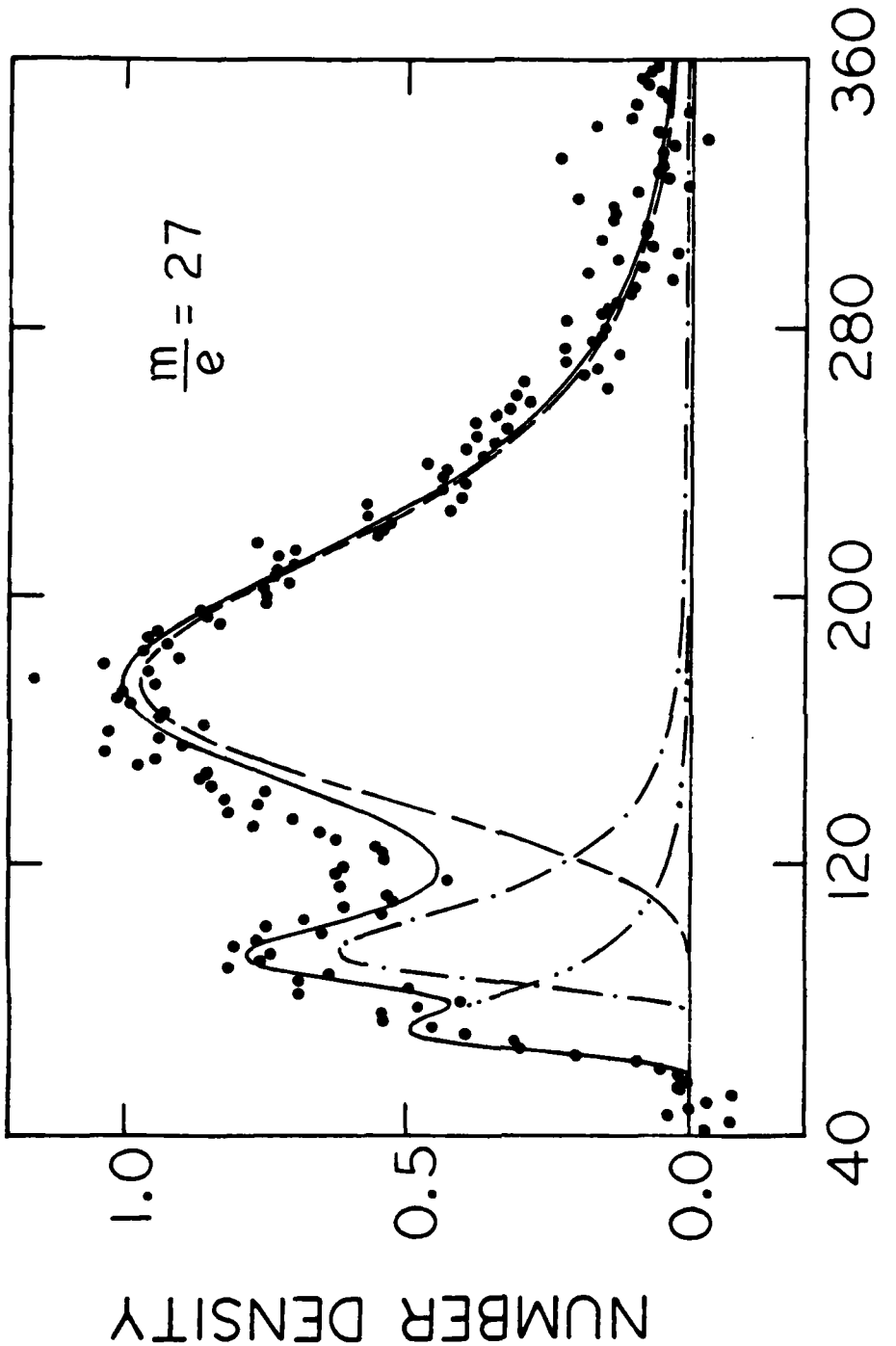

XBL 836-9990

Fig. 7

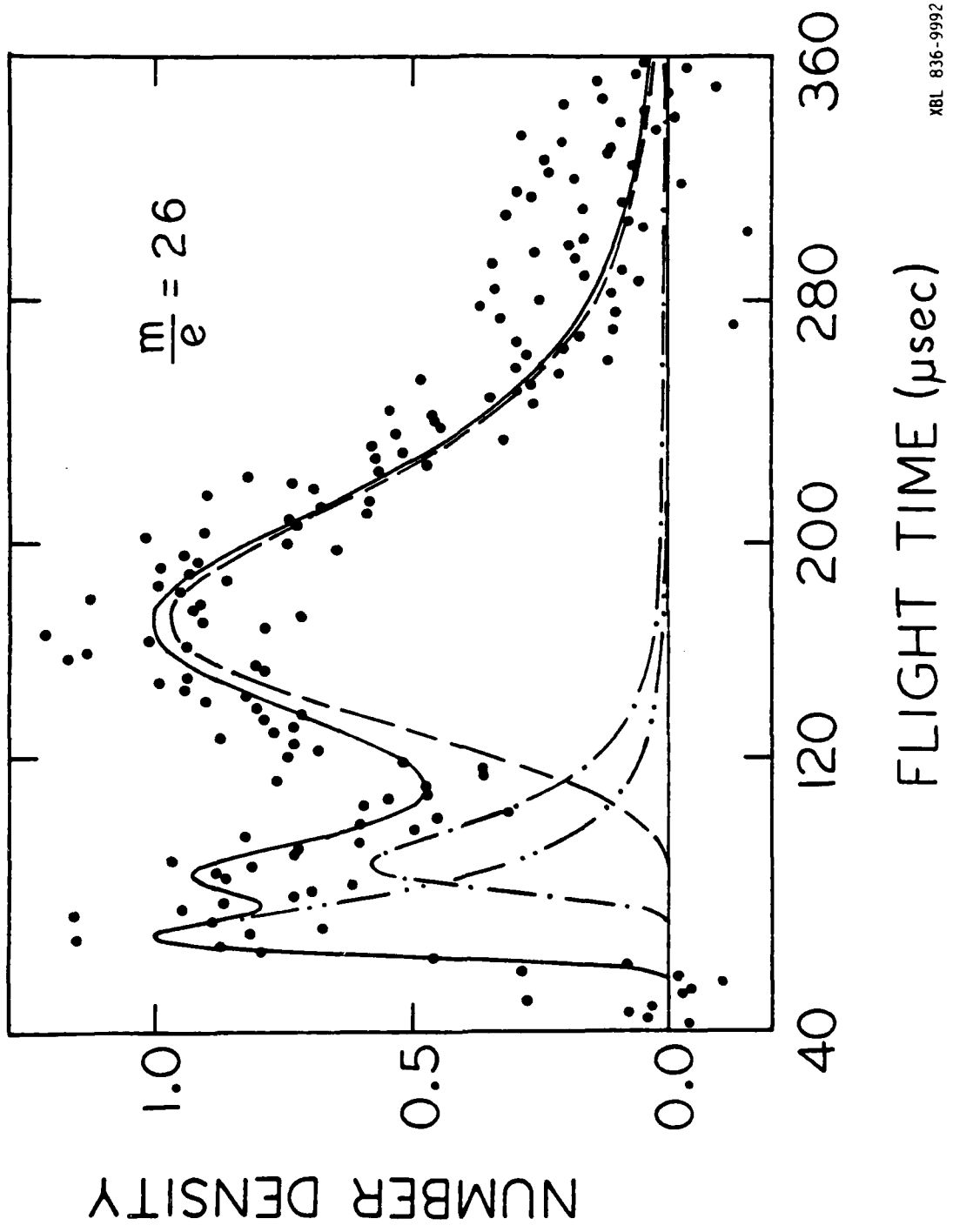
NUMBER DENSITY
1.0
0.5
0.0
40
120
200
280
360
FLIGHT TIME (μsec)
m/e = 26
XBL 836-9992

Fig. 8

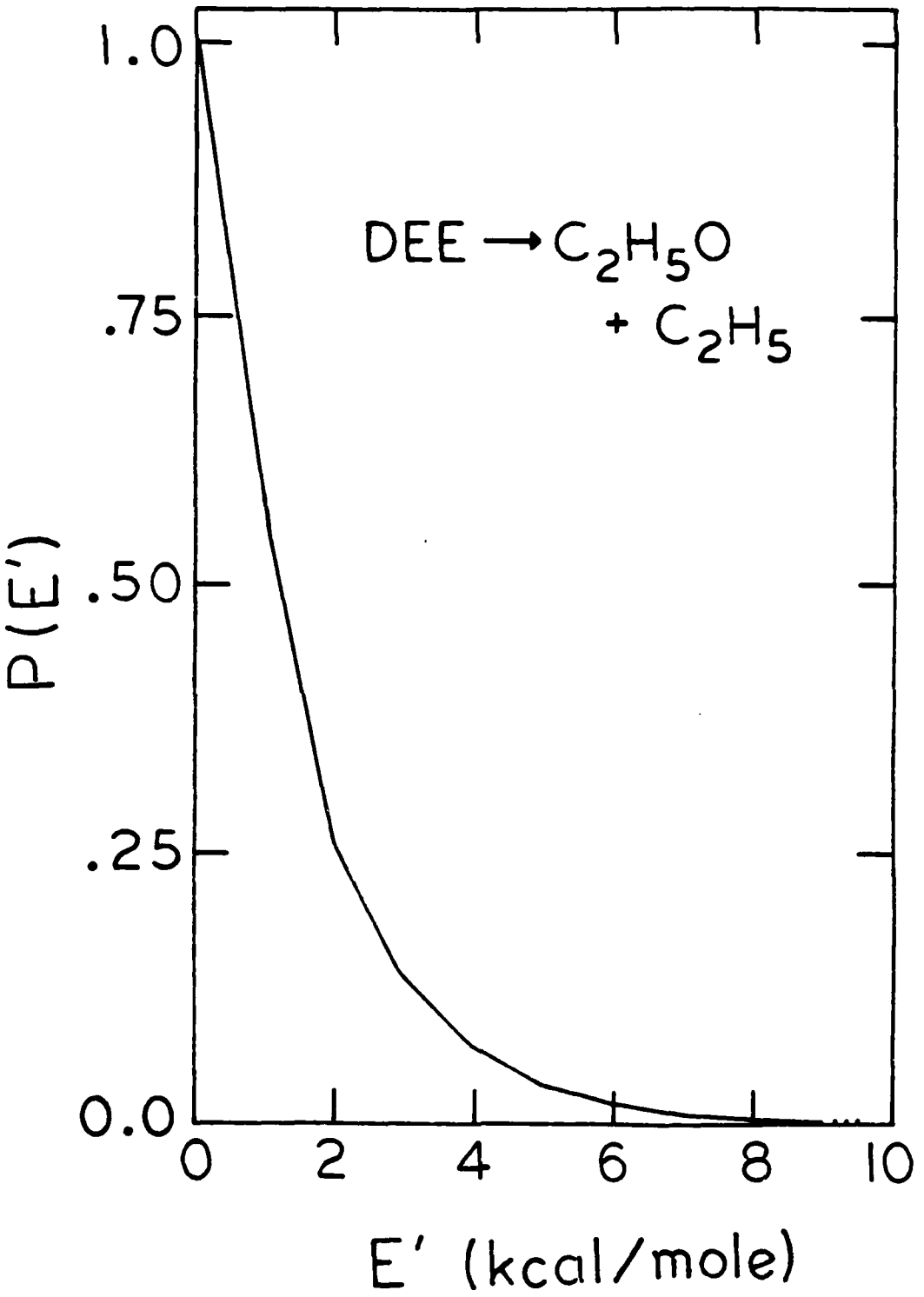

XBL 836-9993

Fig. 9

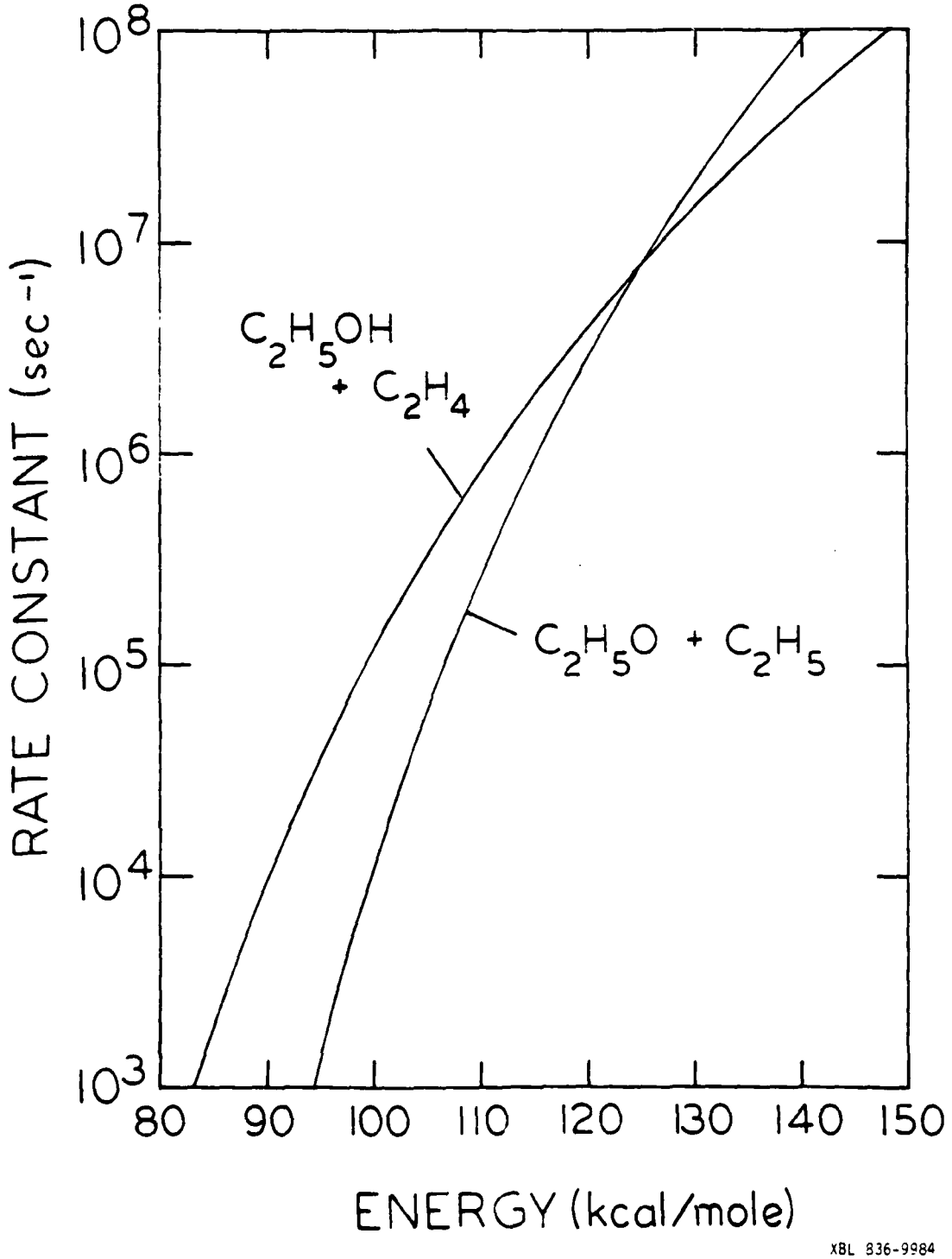
RATE CONSTANT (sec⁻¹)
10⁸
10⁷
10⁶
10⁵
10⁴
10³
C₂H₅OH
+ C₂H₄
C₂H₅O + C₂H₅
80
90
100
110
120
130
140
150
ENERGY (kcal/mole)
XBL 836-9984

Fig. 10

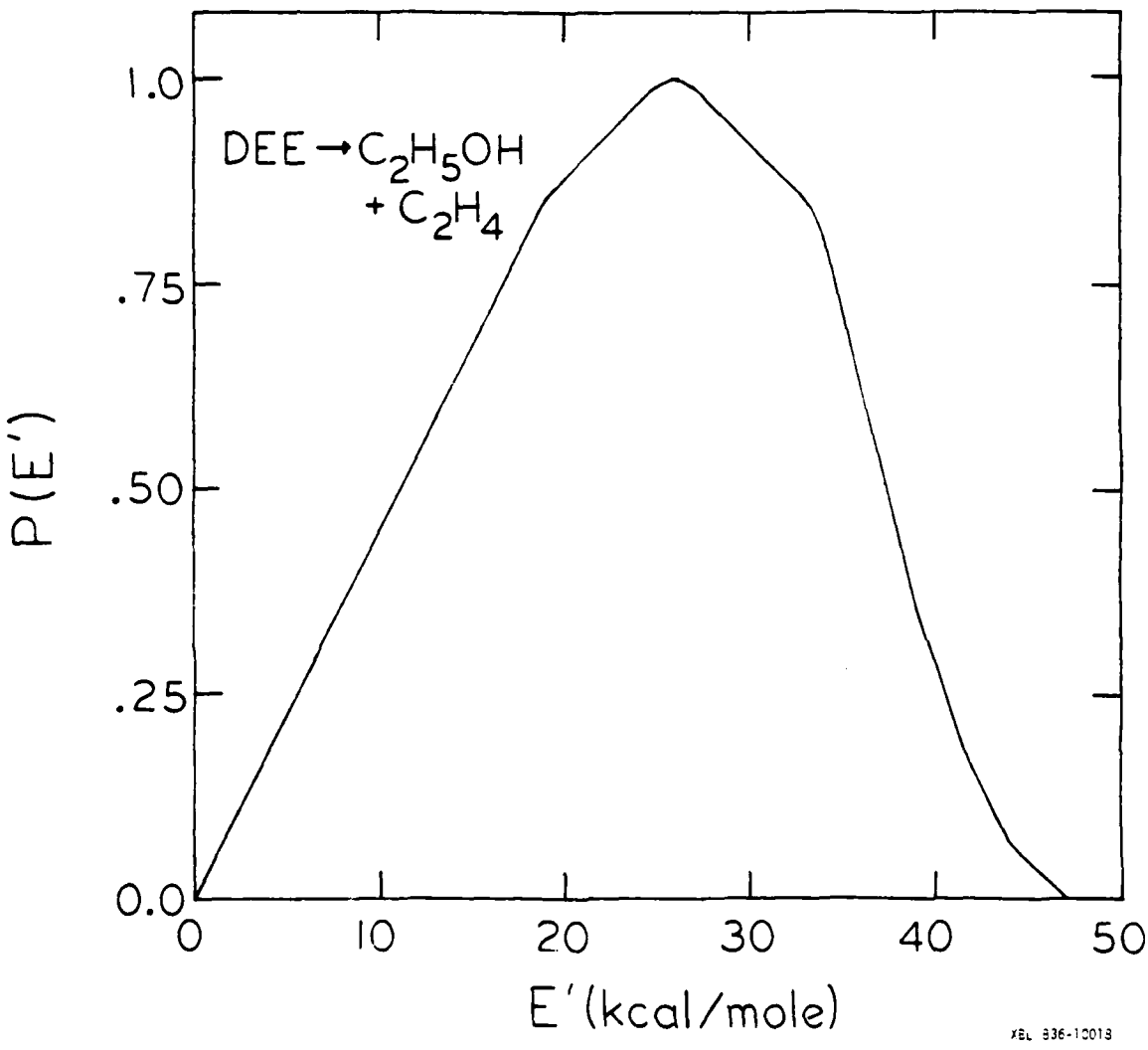
DEE → C_2H_5OH
+ C_2H_4
P(E')
1.0
.75
.50
.25
0.0
0
10
20
30
40
50
E'(kcal/mole)
XBL 836-10018

Fig. 11

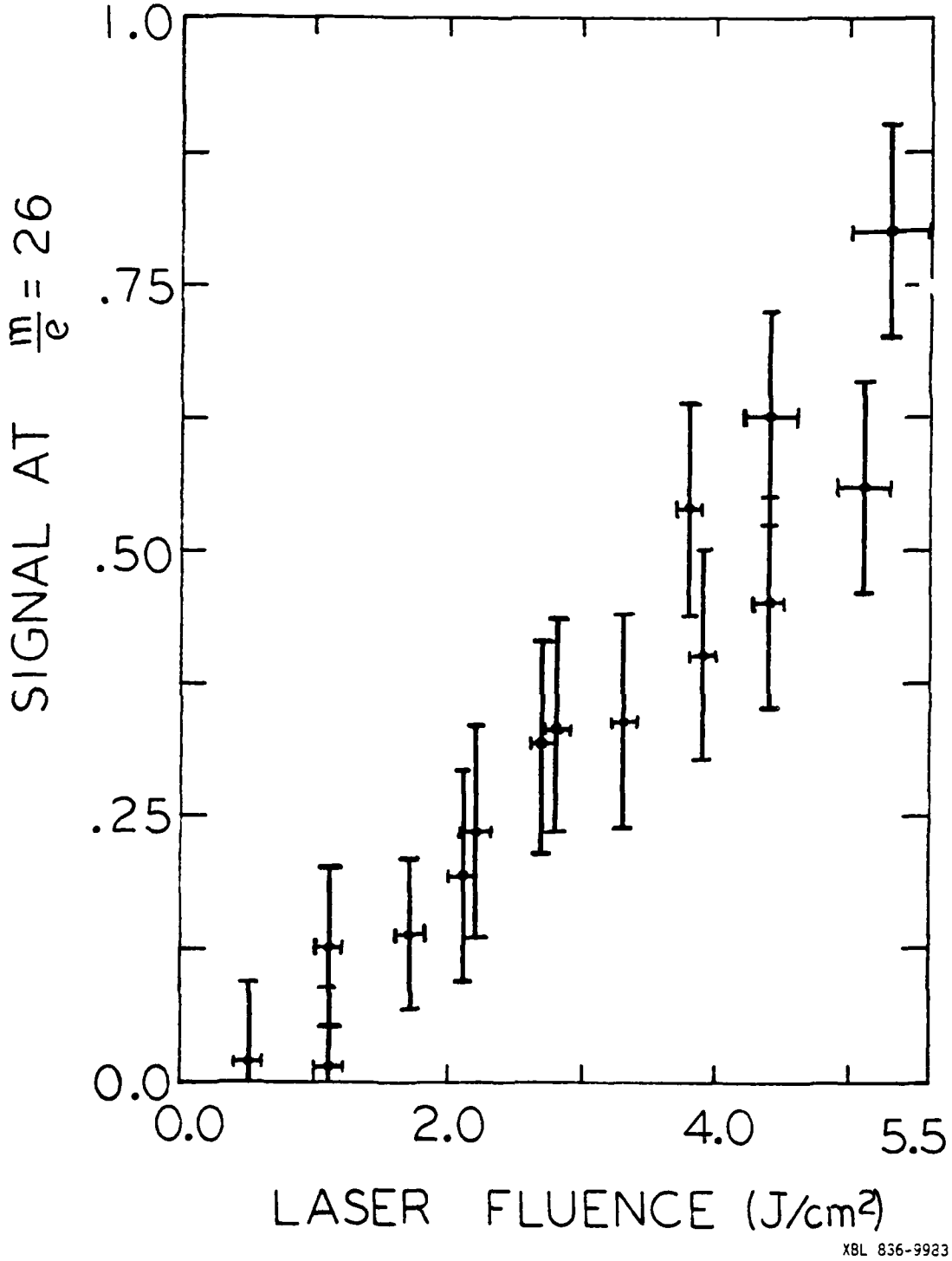
1.0
.75
.50
.25
0.0
SIGNAL AT $\frac{m}{e}$ = 26
0.0
2.0
4.0
5.5
LASER FLUENCE (J/cm²)
XBL 836-9923

Fig. 12

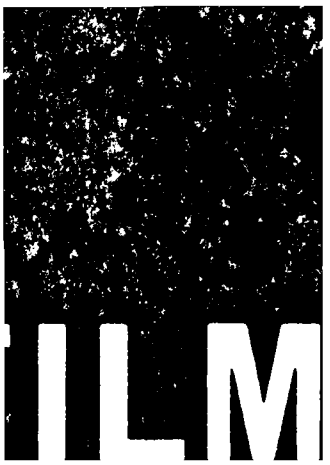
ILM